IEEE Access
Multidisciplinary | Rapid Review | Open Access Journal

SPECIAL SECTION ON ANTENNA AND PROPAGATION FOR 5G AND BEYOND

Received March 12, 2020, accepted March 20, 2020, date of publication March 30, 2020, date of current version April 15, 2020.

Digital Object Identifier 10.1109/ACCESS.2020.2984199

A Dual-Band Dual-Polarized Base Station Antenna Using a Novel Feeding Structure for 5G Communications

QIANG HUA, YI HUANG, (Senior Member, IEEE), AHMED ALIELDIN, (Member, IEEE), CHAOYUN SONG, (Member, IEEE), TIANYUAN JIA, AND XU ZHU, (Senior Member, IEEE)

Department of Electrical and Electronics, University of Liverpool, Liverpool L69 3GJ, U.K.

Corresponding author: Yi Huang (yi.huang@liverpool.ac.uk)

ABSTRACT A dual-band dual-polarized base station antenna for the fifth-generation (5G) mobile system is presented in this paper. The proposed antenna covers the frequency bands from 3.3 to 3.8 GHz (the lower band) and from 4.8 to 5.0 GHz (the upper band) with good isolation between its ports ($\geq$ 20 dB). It consists of two double-oval-shaped dipoles, two double-oval-shaped feeding lines and a cavity reflector. In this design, parts of the dipole antenna structure are used as the feeding lines and it is found that using one arm of the dipole to feed the whole antenna can improve impedance matching. The dual-band performance is achieved by integrating a small oval-shaped loop within the large oval-shaped loop without increasing the size of the radiating patch. The size of the radiating patch is only $0.26\lambda_0 \times 0.26\lambda_0$ (λ_0 is the free-space wavelength at 3.3 GHz). The cavity reflector improves the gain performance and reduces the overall size of the antenna, which is only $0.66\ \lambda_0 \times 0.66\lambda_0 \times 0.2\lambda_0$. The antenna has an average realized gain of 7.56 dBi in the lower band and 7.42 dBi in the higher band. Meanwhile, for both bands, the radiation pattern is stable, and the half power beamwidth is within $65° \pm 5°$. Both simulated and measured results demonstrate that the antenna is a very good candidate for 5G mobile base stations.

INDEX TERMS 5G, base station antenna, coupling feeding, dual-band, dual-polarized.

I. INTRODUCTION

With the rapid development of mobile communication technologies, there is a high demand for base station antennas with better performances to support mobile communication networks. The dual-polarized antenna with high port-to-port isolation and low cross-polarization levels is widely used to increase the signal-to-noise ratio, and channel capacity, combat multipath fading as well as reduce space requirement and installation cost [1]. A general method to create dual-polarization is to use crossed dipoles. To obtain $\pm 45°$ dual-polarization, it is only required to put the crossed dipoles on the diagonals, and it can guarantee the isolation between the antenna units [2]. Furthermore, an increasing number of mobile wireless communication systems use different frequencies, and it is required to use dual or multi-band antennas to reduce occupied space and fabrication cost. It is common that two operating frequency bands are realized at the same antenna [3]–[5]. Quite a few dual-band dual-polarized antennas have been proposed [6]–[8]. They are mainly designed and applied for 2G/3G/LTE applications. With the rapid increase of communication data capacity, the fifth-generation (5G) mobile communication system is being deployed from this year. In 2016, the European Commission (EC) declared that the band from 3.4 to 3.8 GHz would be used for 5G trials. In 2017, China's Ministry of Industry and Information Technology (MIIT) officially announced that 3.3 – 3.4 (indoor only), 3.4 – 3.6 and 4.8 – 5.0 GHz bands were allocated for 5G services [9]. Therefore, it is essential to design a dual-polarized base station antenna, which covers the bands of 3.3 – 3.8 GHz and 4.8 – 5.0 GHz.

At the moment, many dual-polarized base station antennas have already been designed and fabricated using different feeding lines for 2G/3G/LTE applications, and then a wider impedance bandwidth can be achieved, such as Y-shaped feeding lines [10], T-shaped feeding lines [11], branch-shaped feeding lines [12] and arc-shaped feeding lines [13]. Therefore, choosing a suitable feeding line should be considered in the design process. In this design, part of the dipole antenna structure is utilized as the feeding lines to

The associate editor coordinating the review of this manuscript and approving it for publication was Qammer Hussain Abbasi.

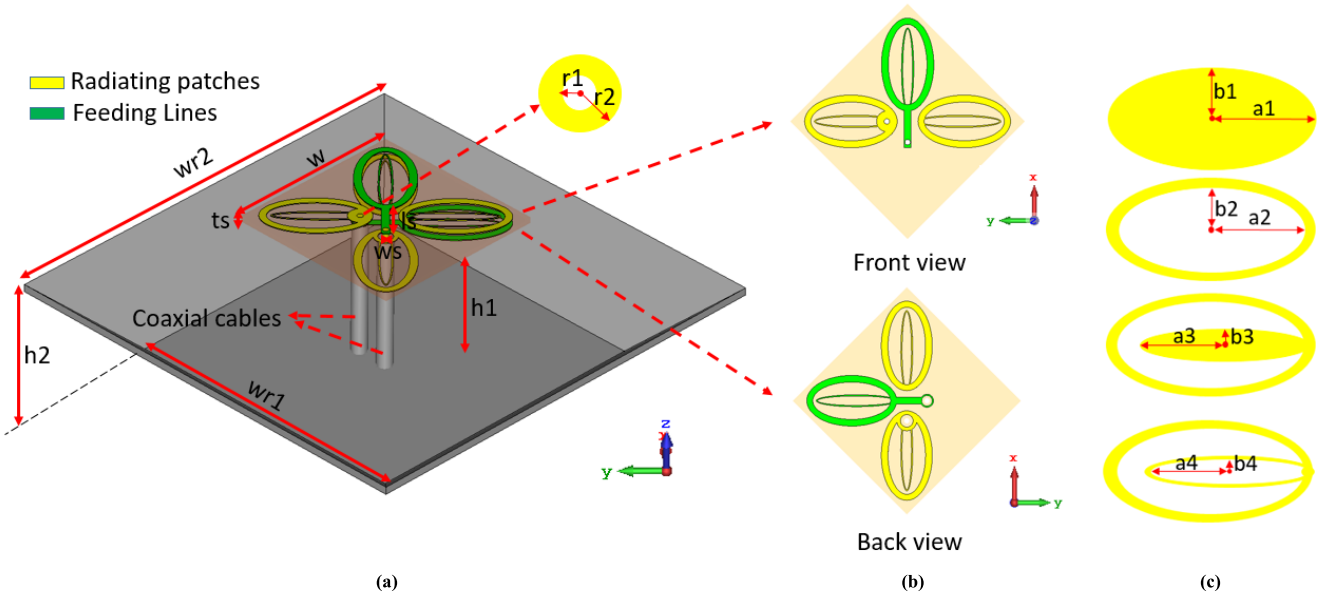

FIGURE 1. The geometry of the proposed antenna. (a) 3-D view. (b) Front view and back view of the radiator. (c) Detailed structure of radiating patches.

feed the complete dipole. Meanwhile, it is found that using one arm of the dipole to feed the whole antenna can achieve an optimum impedance matching.

In this paper, a dual-band dual-polarized antenna for 5G base station is proposed. The two operating bands are achieved by a double-oval-shaped dipole radiator. By putting two crossed dipoles on the diagonal lines, the $\pm$ 45° dual polarization is easily achieved. In addition, the double-oval-shaped feeding line is utilized to achieve an optimum impedance matching. The proposed antenna achieves a stable radiation pattern and half power beamwidth (HPBW) over the two operation bands. Moreover, the radiating patch is only $0.26\lambda_0 \times 0.26\lambda_0$, which is small for the frequency band.

The organization of this paper is as follows. The configuration and optimization of the proposed antenna are introduced in Section II. The simulated and measured results are presented and discussed in Section III. Finally, conclusions are drawn in Section IV.

II. ANTENNA DESIGN

A. THE GEOMETRY OF THE PROPOSED ANTENNA

The geometry of the proposed antenna is shown in Fig. 1, and the optimum parameters related to antenna design are listed in Table 1. The antenna is composed of two double-oval-shaped dipoles, two double-oval-shaped feeding lines and a cavity reflector. The dipoles and feeding lines are printed on a thin (0.8 mm) FR-4 substrate with a relative permittivity of 4.4 and a loss tangent of 0.02 around 3 GHz. Two crossed double-oval-shaped dipoles are printed along the diagonals of the substrate to achieve $\pm$ 45° dual-polarization. Each double-oval-shaped radiating patch includes two parts, an outer oval-shaped loop and an inner oval-shaped loop. The inner oval-shaped loop is used to control the operating frequency of the upper band, while the outer oval-shaped loop is used to control the operating frequency of the lower band. Each dipole and its corresponding feeding line are printed on the opposite sides of the substrate, as shown in Fig. 1. Utilizing this configuration, the intersection between the feeding lines is avoided, which makes it easy for fabrication and provide high isolation between the feeding ports. Each dipole is fed by a coaxial cable. For the horizontal dipole, the inner of the coaxial cable is connected to one arm of the dipole, and the outer of the dipole is connected to the corresponding feeding line through the substrate. For the vertical dipole, the inner of the coaxial cable is connected to the corresponding feeding line, and the outer of the coaxial cable is connected to one arm of the dipole through the substrate. Therefore, two holes are drilled in the substrate for connection. Instead of using a square-shaped reflector, a cavity reflector is chosen in the proposed antenna to achieve higher gain and reduce the overall size of the antenna.

TABLE 1. Parameters of the proposed antenna.

Parameter	Value (mm)	Parameter	Value (mm)	Parameter	Value (mm)
a1	6.9	*a4*	5.6	*wr2*	60
b1	3.8	*b4*	0.7	*h1*	18
a2	6	*r1*	0.8	*h2*	10
b2	2.8	*r2*	1	*ws*	1
a3	5.8	*w*	24	*ls*	3.9
b3	0.9	*wr1*	40	*ts*	0.8

B. IMPEDANCE MATCHING

To describe the principle of the impedance matching more conveniently, the impact of the coupling between the two

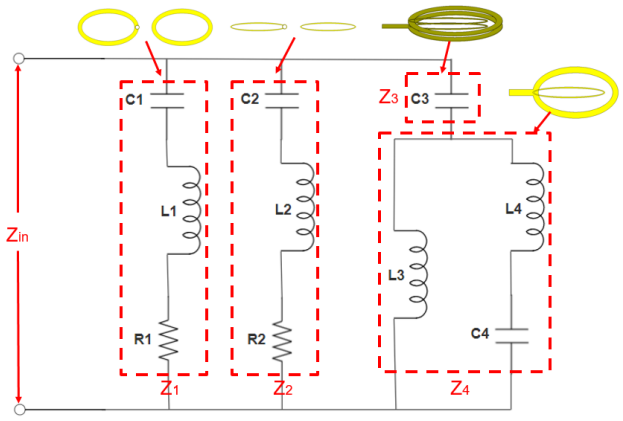

FIGURE 2. The equivalent circuit of the proposed antenna.

dipoles are ignored here. The circuit is obtained by dividing the whole antenna into three parts, including the inner oval-shaped loop, outer oval-shaped loop and feeding line. The inner and outer oval-shaped loop can be considered as two parallel dipoles. They are simply represented as Z_1 and Z_2. The feeding line consists of both inner and outer oval-shaped loop, each loop can be represented as the inductance (L3 and L4) and they are parallel connected. There is a coupling (C4) between the two loops. The coupling between the dipole antenna and the feeding line is considered as Z_3. Therefore, the equivalent circuit of proposed antenna can be obtained as shown in Fig. 2.

From Fig. 2, we can get

$$Z_1 = \frac{1}{j\omega C_1} + j\omega L_1 + R_1 \tag{2-1}$$

$$Z_2 = \frac{1}{j\omega C_2} + j\omega L_2 + R_2 \tag{2-2}$$

$$Z_3 = \frac{1}{j\omega C_3} \tag{2-3}$$

$$Z_4 = \frac{j\omega L_3 \cdot (j\omega L_4 + \frac{1}{j\omega C_4})}{j\omega L_3 + j\omega L_4 + \frac{1}{j\omega C_4}} \tag{2-4}$$

$$Z_{in} = \frac{Z_1 \cdot Z_2 \cdot (Z_3 + Z_4)}{Z_1 \cdot Z_2 + Z_1 \cdot (Z_3 + Z_4) + Z_2 \cdot (Z_3 + Z_4)} \tag{2-5}$$

where Z_1 is the impedance of the outer oval-shaped loop dipole, Z_2 is the impedance of the inner oval-shaped loop dipole, Z_3 is the coupling between the feeding line and the dipole, Z_4 is the impedance of the feeding line, and Z_{in} is the input impedance of the antenna. The resonant frequency is determined by the inner and outer oval-shaped loop of the dipole (Z_1 and Z_2). The feeding line can be considered as a capacitive feed method, which can improve the impedance matching of antenna significantly. The parallel inductances (L3 and L4) and capacitance (C4) have been optimized to broaden the bandwidth of the proposed antenna by changing the length of the feeding line, which will be shown later.

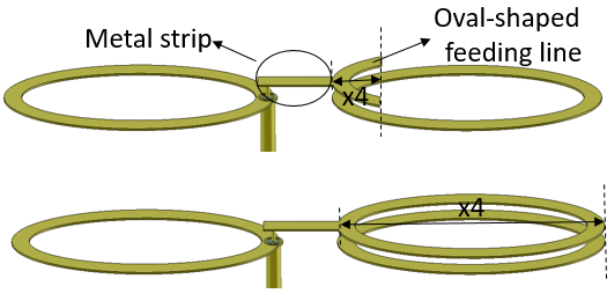

FIGURE 3. The coupling feeding structure (with reflector).

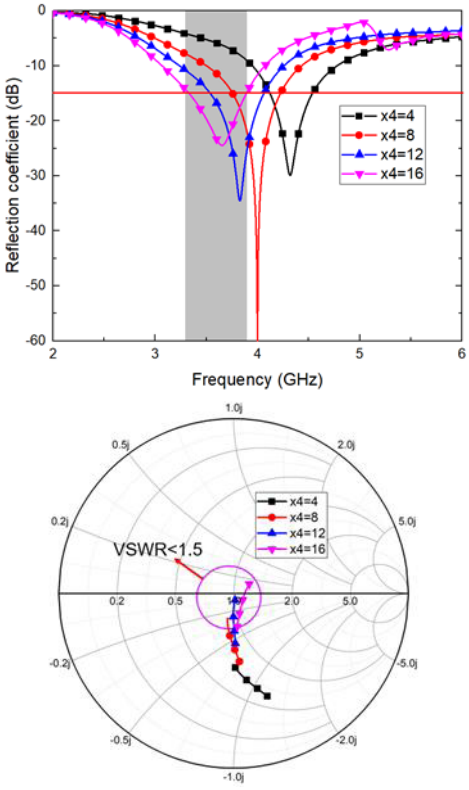

FIGURE 4. The effect of x4 on the reflection coefficient illustrated by reflection coefficient and Smith chart.

C. OVAL-SHAPED FEEDING LINE

In this design, a new feeding structure is introduced. Instead of considering the structure of the feeding line, the new feeding line looks like part of the dipole, is utilized to couple the whole dipole, as shown in Fig. 3. The inner of the coaxial cable is connected to the metal strip through the substrate, which is part of the feeding line. The length of the oval-shaped feeding line is represented as x4. With the increase of x4, the resonant frequency moves to the lower band, and the bandwidth of the operating frequency almost keep the same, as shown in Fig. 4. Meanwhile, x4 also determines the coupling between the dipole and feeding line and hence affects the input impedance of the antenna. As shown in the Smith chart in Fig. 4, it is obvious that the input impedance becomes

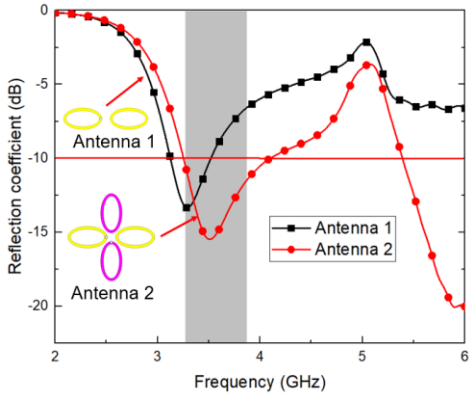

FIGURE 5. The geometry and reflection coefficient of Antenna 1 and Antenna 2.

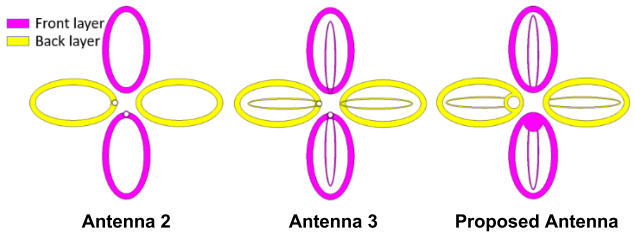

FIGURE 6. The evolution of the proposed antenna.

more inductive when the length of x4 gets closer to the length of one arm of the dipole and vice versa. The optimum impedance matching is achieved when the length of x4 is the same as the length of one arm of the dipole. In addition, the reflection coefficient is less than −15 dB within the desired frequency band.

D. EVOLUTION OF THE PROPOSED ANTENNA

Fig. 5 shows the geometry of Antenna 1 and Antenna 2. Antenna 1 is a simple dipole, and Antenna 2 is two crossed dipoles. For crossed dipoles, when one dipole is driven, the other dipole works as a parasitic element and can improve the impedance matching through the coupling, as shown in Fig. 5. Therefore, when designing the elements for crossed dipoles, both driven dipole and un-driven dipole should be considered.

The evolution of the proposed dual-band antenna is presented in Fig. 6. Initially, the dipole antenna only consists of an outer oval-shaped loop. The outer oval-shaped loop provides a resonant frequency for the lower band. The main parameters of the oval shape are the semi-major and semi-minor axes. When ignore the influence of the coupling between two dipoles, the resonant frequency of the dipole is affected by the length of semi-major axis, when the length of the semi-minor axis is fixed, as shown in Fig. 7. To be specific, the resonant frequency moves to the lower frequency band with the increase of the length of semi-major axis, while the bandwidth keeps the same. When the length of the semi-major axis is fixed, the bandwidth of the antenna

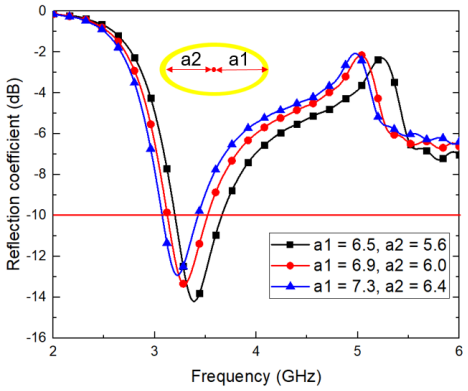

FIGURE 7. The influence of the length of semi-major axis on reflection coefficient (with reflector).

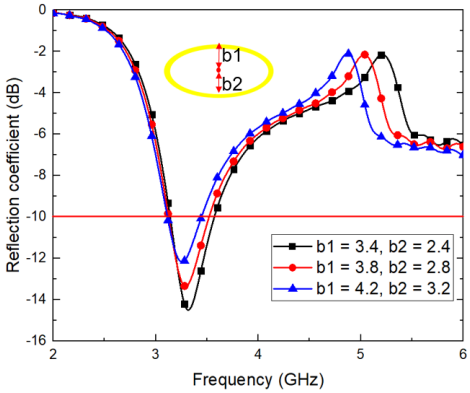

FIGURE 8. The influence of the length of semi-minor axis on reflection coefficient (with reflector).

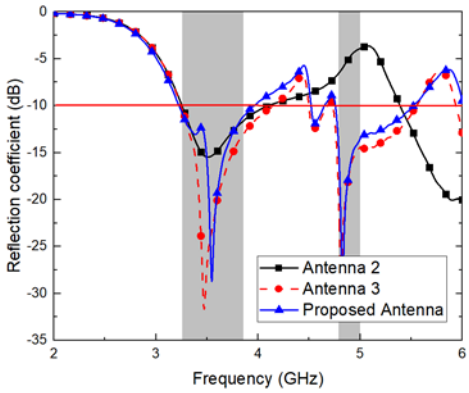

FIGURE 9. The reflection coefficient of the Antenna 2, Antenna 3 and Proposed antenna.

is broadened with the increase of the length of semi-minor axis. Meanwhile, it has little effect on the resonant frequency, as shown in Fig. 8. Therefore, there is a trade-off between the size and the bandwidth.

Antenna 2 cannot provide resonant frequency between 4.8 and 5.0 GHz, as shown in Fig. 9. Therefore, an inner oval-shaped loop is introduced and integrated within the outer oval-shaped, which is shown as Antenna 3 in Fig. 9.

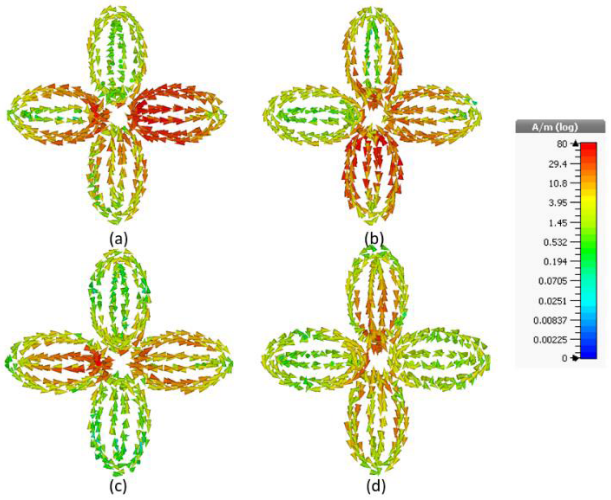

FIGURE 10. The current distribution (a) port 1 is driven at 3.55 GHz. (b) port 2 is driven at 3.55 GHz. (c) port 1 is driven at 4.9 GHz. (d) port 2 is driven at 4.9 GHz.

FIGURE 11. Two different shapes of the reflector. (a) square-shaped reflector. (b) cavity reflector.

It provides an operating frequency band covering 4.8 – 5.0 GHz. Then, the dual-band antenna is achieved without increasing the size of the antenna. Finally, a circular ring is introduced and integrated with one arm of the dipole. It is utilized to provide enough space for soldering the coaxial cable with the antenna, and it has little effect on the antenna performance, as shown in Fig. 9.

Fig. 10 depicts the current distribution of the proposed antenna at different frequencies when the two ports are driven. For the lower band, the outer oval-shaped loop of driven dipole has the major current intensity distribution. For the upper band, the inner oval-shaped loop of driven dipole has the major current intensity. For both two bands, the other dipole, which is not driven works as a parasitic element and has less current intensity distribution.

E. CAVITY REFLECTOR

Fig. 11 shows two different structures of the reflector, and they are square-shaped reflector and cavity reflector. Normally, the reflector used for base station antennas is square-shaped because it is easy for fabrication. In this design, the cavity reflector is used to decrease the size of the whole antenna. Meanwhile, it can also improve the realized gain of the proposed antenna, especially for the higher frequency band, as shown in Fig. 12. This happens because the beamwidth of the proposed antenna becomes narrow by using the cavity reflector, which is more obvious for the higher frequency band, as shown in Fig. 12. However, it is still

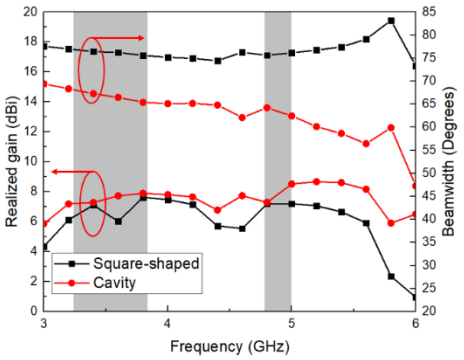

FIGURE 12. The realized gain and beamwidth of the square-shaped and cavity reflector.

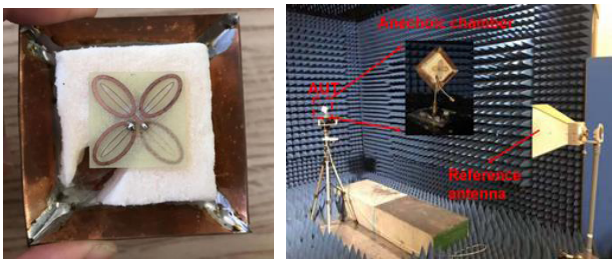

FIGURE 13. The fabricated antenna and antenna under measurement.

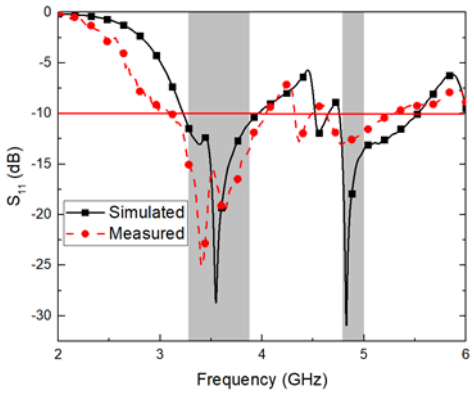

FIGURE 14. The simulated and measured reflection coefficient.

acceptable for base station applications. In addition, the cavity reflector provides a good radiation pattern for both lower and higher band, which will be shown later.

III. ANTENNA PERFORMANCE

The simulation results were obtained using CST microwave studio. To verify the simulation results, the proposed base station antenna was fabricated and measured, as shown in Fig. 13. Fig. 13 also depicts the setup of the measurement; it is accomplished in an anechoic chamber using a Vector Network Analyzer (VNA). Finally, the measurement results of S-parameters, gain, and radiation pattern are obtained.

Fig. 14 illuminates the simulated and measured reflection coefficients of the proposed antenna. The reflection

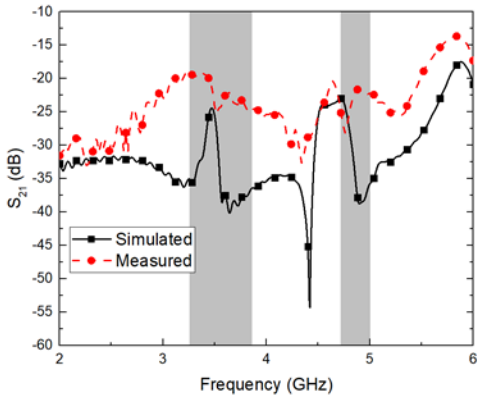

FIGURE 15. The simulated and measured port-to-port isolation.

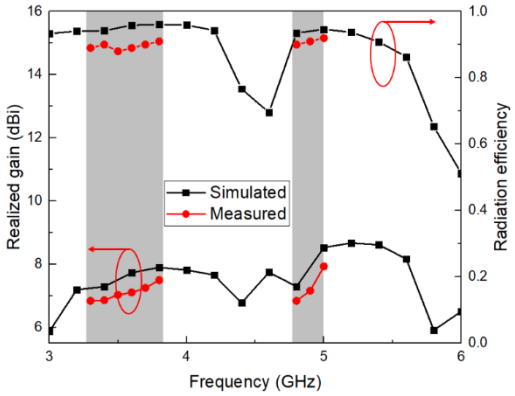

FIGURE 16. The simulated and measured realized gain and radiation efficiency.

coefficients for the desired frequency bands 3.3 – 3.8 GHz and 4.8 – 5.0 GHz are less than −10 dB. The deviation between the simulated and measured reflection coefficients may be due to fabrication tolerance and soldering problem.

Fig. 15 shows the simulated and measured port-to-port isolation of the proposed antenna. Both the simulated and measured port-to-port isolation are better than 20 dB, which provide good isolation for the base station applications.

The simulated and measured realized gain and radiation efficiency are shown in Fig. 16. The lower band has an average gain of 7.56 dBi, and the higher band has an average gain of 7.42 dBi within the frequency band. Meanwhile, the overall radiation efficiency of proposed antenna is around 90%.

The simulated and measured co- and cross-polarized radiation patterns at the start and end frequencies of each band in H-plane (XZ plane) and V-plane (YZ-plane) are illuminated in Fig. 18. It shows a good agreement between the simulated and measured results. Moreover, the radiation pattern is stable for both bands. The cross-polarization discrimination ratio (XPD) at boresight is better than 25 dB for both bands. The HPBW for both bands is within 65 ± 5°, as shown in Fig. 19, which is suitable for base station applications.

A comparative study between the proposed antenna and previous designs is given in Table 2. The proposed antenna

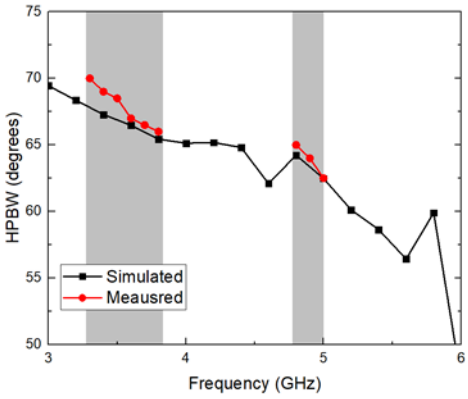

FIGURE 17. The simulated and measured HPBW.

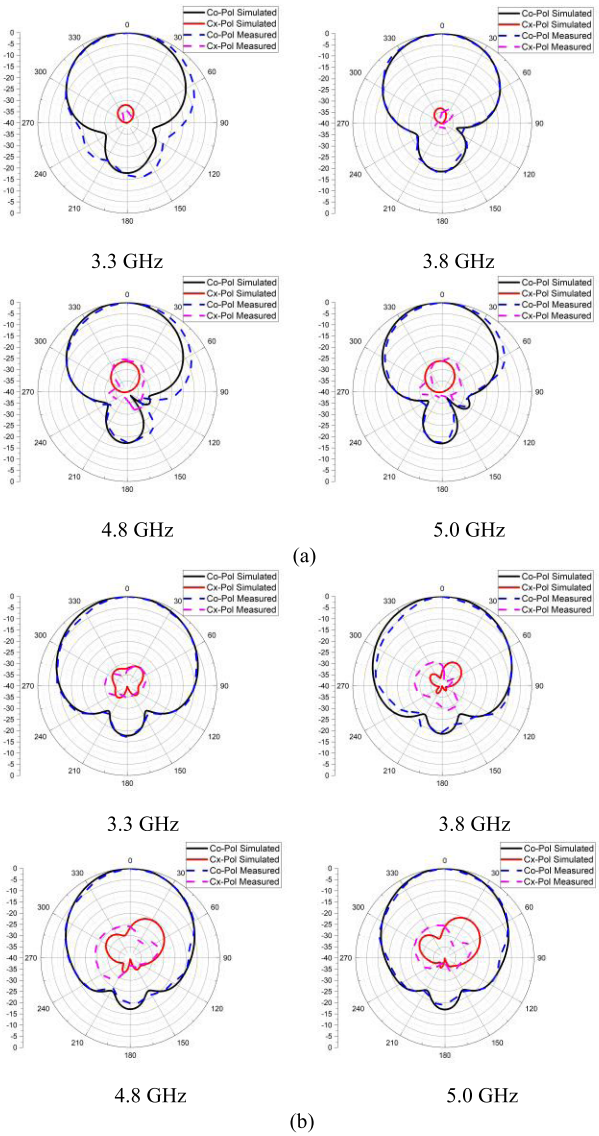

FIGURE 18. The simulated co- and cross-polarized radiation pattern in (a) V-plane. (b) H-plane.

can be easily fabricated and provide a dual-band performance with a relatively small size. It also has a good cross-polarization and with acceptable gains and isolation.

TABLE 2. Comparison of various characteristics of the proposed antenna with several antennas.

Reference	Frequency band (GHz)	Bands	Polarization	Isolation (dB)	Average gain (dBi)	Size (mm^3)	XPD (dB)	Design Complexity
[14]	3.65 – 3.81	Single	Dual	31	10	86 × 81 × 3	23	Complex
[15]	3.3 – 3.6	Single	Dual	28.8	8.2	72 × 72 × 18.8	24	Easy
[16]	3.4 – 3.8	Single	Dual	23	9	-	25	Complex
[17]	3.3 – 3.6	Single	Dual	25	7.3	72 × 72 × 18.3	24.5	Complex
[18]	3.28 – 3.7 & 4.75 – 5.0	Dual	Dual	40	8 & 10	50 × 50 × 7.4	-20	Complex
Proposed	**3.3 – 3.8 & 4.8 – 5.0**	**Dual**	**Dual**	**20**	**7.56 & 7.42**	**60 × 60 × 18**	**25**	**Easy**

IV. CONCLUSION

In this paper, a novel dual-band dual-polarized antenna for 5G base station has been designed, made and tested. Using a double-oval-shaped dipole, the dual-band performance has been achieved without increasing the size of the antenna. A new feeding structure has been introduced, which uses part of the dipole antenna as feeding lines, to couple the whole dipole and provides an improved impedance matching. The cavity reflector has been employed to offer a higher gain and reduce the overall size of the antenna. In addition to easy fabrication and low profile, the proposed antenna also has a stable gain, high XPD and high isolation between the two ports. The proposed antenna has been fabricated and measured. The measured results have shown a good agreement with the simulated results and demonstrated that the proposed antenna is indeed a very good candidate for 5G mobile base stations.

REFERENCES

[1] H. Li, L. Kang, F. Wei, Y.-M. Cai, and Y.-Z. Yin, "A low-profile dual-polarized microstrip antenna array for dual-mode OAM applications," *IEEE Antennas Wireless Propag. Lett.*, vol. 16, pp. 3022–3025, 2017.

[2] Y. Luo, Q.-X. Chu, and D.-L. Wen, "A Plus/Minus 45 degree dual-polarized base-station antenna with enhanced cross-polarization discrimination via addition of four parasitic elements placed in a square contour," *IEEE Trans. Antennas Propag.*, vol. 64, no. 4, pp. 1514–1519, Apr. 2016.

[3] Z. Wang, G.-X. Zhang, Y. Yin, and J. Wu, "Design of a dual-band high-gain antenna array for WLAN and WiMAX base station," *IEEE Antennas Wireless Propag. Lett.*, vol. 13, pp. 1721–1724, 2014.

[4] W. X. An, H. Wong, K. L. Lau, S. F. Li, and Q. Xue, "Design of broadband dual-band dipole for base station antenna," *IEEE Trans. Antennas Propag.*, vol. 60, no. 3, pp. 1592–1595, Mar. 2012.

[5] A. Bashiri and K. Forooraghi, "Dual band dual polarized conformai microstrip array for base stations," in *Proc. 24th Iranian Conf. Electr. Eng. (ICEE)*, May 2016, pp. 1640–1644.

[6] Y. He, Z. Pan, X. Cheng, Y. He, J. Qiao, and M. M. Tentzeris, "A novel dual-band, dual-polarized, miniaturized and low-profile base station antenna," *IEEE Trans. Antennas Propag.*, vol. 63, no. 12, pp. 5399–5408, Dec. 2015.

[7] Y. Wang and Z. Du, "Dual-polarized dual-band microstrip antenna with similar-shaped radiation pattern," *IEEE Trans. Antennas Propag.*, vol. 63, no. 12, pp. 5923–5928, Dec. 2015.

[8] A. Alieldin, Y. Huang, S. J. Boyes, M. Stanley, S. D. Joseph, and B. Al-Juboori, "A dual-broadband dual-polarized fylfot-shaped antenna for mobile base stations using MIMO over-lapped antenna subarrays," *IEEE Access*, vol. 6, pp. 50260–50271, 2018.

[9] *Ministry of Industry and Information Technology of China. [EB/OL].* [Online]. Available: http://www.miit.gov.cn/n1146290/n4388791/c5906943/content.html

[10] Q. Chu, D. Wen, and Y. Luo, "A broadband ±45° dual-polarized antenna with Y-shaped feeding lines," *IEEE Trans. Antennas Propag.*, vol. 63, no. 2, pp. 483–490, Feb. 2015.

[11] D.-Z. Zheng and Q.-X. Chu, "A wideband dual-polarized antenna with two independently controllable resonant modes and its array for base-station applications," *IEEE Antennas Wireless Propag. Lett.*, vol. 16, pp. 2014–2017, 2017.

[12] R. Wu and Q.-X. Chu, "Multi-mode broadband antenna for 2G/3G/LTE/5G wireless communication," *Electron. Lett.*, vol. 54, no. 10, pp. 614–616, May 2018.

[13] X.-W. Xiao, Y.-D. Kong, and Q.-X. Chu, "An oval-shaped broadband ±45° dual-polarized base station antenna for 2G/3G/LTE applications," in *Proc. 6th Asia–Pacific Conf. Antennas Propag. (APCAP)*, Oct. 2017, pp. 1–3.

[14] Y. Gao, R. Ma, Y. Wang, Q. Zhang, and C. Parini, "Stacked patch antenna with dual-polarization and low mutual coupling for massive MIMO," *IEEE Trans. Antennas Propag.*, vol. 64, no. 10, pp. 4544–4549, Oct. 2016.

[15] Q. Wu, P. Liang, and X. Chen, "A broadband ±45° dual-polarized multiple-input multiple-output antenna for 5G base stations with extra decoupling elements," *J. Commun. Inf. Netw.*, vol. 3, no. 1, pp. 31–37, Mar. 2018.

[16] C. Hua, R. Li, Y. Wang, and Y. Lu, "Dual-polarized filtering antenna with printed jerusalem-cross radiator," *IEEE Access*, vol. 6, pp. 9000–9005, 2018.

[17] H. Huang, X. Li, and Y. Liu, "5G MIMO antenna based on vector synthetic mechanism," *IEEE Antennas Wireless Propag. Lett.*, vol. 17, no. 6, pp. 1052–1055, Jun. 2018.

[18] B. Feng, L. Li, J.-C. Cheng, and C.-Y.-D. Sim, "A dual-band dual-polarized stacked microstrip antenna with high-isolation and band-notch characteristics for 5G microcell communications," *IEEE Trans. Antennas Propag.*, vol. 67, no. 7, pp. 4506–4516, Jul. 2019.

QIANG HUA received the B.Sc. degree in communication engineering from the University of Liverpool, Liverpool, U.K., in 2016, and the M.Sc. degree in digital signal processing from The University of Manchester, Manchester, U.K., in 2017. He is currently pursuing the Ph.D. degree in base station antennas with the University of Liverpool. His current research focuses on the base station antenna design for 5G in wireless communications.

YI HUANG (Senior Member, IEEE) received the B.Sc. degree in physics from Wuhan University, China, in 1984, the M.Sc. (Eng.) degree in microwave engineering from NRIET, Nanjing, China, in 1987, and the D.Phil. degree in communications from the University of Oxford, U.K., in 1994. He has been conducting research in the areas of wireless communications, applied electromagnetics, radar, and antennas, since 1987. His experience includes three years spent with NRIET as a Radar Engineer and various periods with the Universities of Birmingham, Oxford, and Essex, U.K., as a Member of Research Staff. He worked as a Research Fellow at British Telecom Laboratories, in 1994, and then joined the Department of Electrical Engineering and Electronics, University of Liverpool, U.K., as a Faculty Member, in 1995, where he is currently a

Full Professor in wireless engineering, the Head of the High Frequency Engineering Group, and the Deputy Head of the Department. He has published over 350 refereed articles in leading international journals and conference proceedings, and authored *Antennas: From Theory to Practice* (John Wiley, 2008) and *Reverberation Chambers: Theory and Applications to EMC and Antenna Measurements* (John Wiley, 2016). He is a Fellow of IET and Senior Fellow of HEA. He has received many research grants from research councils, government agencies, charity, EU, and industry, acted as a consultant to various companies, and served on a number of national and international technical committees and been an editor, an associate editor, or a guest editor of five international journals. He has been a keynote/invited speaker and organizer of many conferences and workshops (e.g., WiCom 2006, 2010, IEEE iWAT2010, LAPC2012, and EuCAP2018). He is currently the Editor-in-Chief of *Wireless Engineering and Technology*, an Associate Editor of the IEEE Antennas and Wireless Propagation Letters, U.K., and an Ireland Representative to European Association of Antenna and Propagation (EurAAP).

AHMED ALIELDIN (Member, IEEE) received the B.Sc. degree in radar engineering from the Military Technical College, Egypt, in 2005, the M.Sc. (Eng) degree in antenna and microwave propagation from the University of Alexandria, Egypt, in 2013, and the Ph.D. degree in antennas and electromagnetics from the University of Liverpool, U.K., in 2019.

His academic research activities and Ph.D. were centered on antenna designing and measurements with an emphasis on mobile communication applications. His academic research work covered novel textile antennas, multiple-input multiple-output antennas, base station antennas, satellite antennas, transparent antennas, and phased-MIMO radar antennas.

In addition to work in academia, he also held various positions throughout more than ten years working in the industry. He currently works as a Senior RF Research Scientist with Benha Electronics Company, where he is involved in projects of national importance. He has authored/coauthored many articles in leading international journals and conference proceedings. He has also filed a patent. He serves as a technical reviewer for leading academic journals and conferences and served as the session chair in many international conferences.

CHAOYUN SONG (Member, IEEE) received the B.Eng., M.Sc., and Ph.D. degrees in electrical engineering and electronics from the University of Liverpool (UoL), Liverpool, U.K., in 2012, 2013, and 2017, respectively. He was a Postdoctoral Research Associate with UoL, from 2017 to 2020. He is currently an Assistant Professor with the School of Engineering and Physical Sciences (EPS), Heriot-Watt University, Edinburgh, U.K. He has published more than 60 articles (including 30 IEEE Transactions) in peer-reviewed journals and conference proceedings. He has held two U.S. patents and two U.K. patents. His current research interests include wireless energy harvesting and wireless power transfer technologies, antennas and microwave circuits using novel materials, dielectric material and ionic liquids in RF applications, metamaterials and meta-surfaces in RF, energy harvesting, and sensing technologies. He was a recipient of many international awards, such as the BAE Systems Chairman's Award, in 2017, for the innovation of next generation global navigation satellite system antennas. In 2018, he received the highly-commended award from the prestigious IET Innovation Awards over three categories: Energy and Power, Emerging Technologies, and Young Innovators. He has been a Regular Reviewer of more than 25 international journals, including *Nature Communications*, *Applied Physics Letters*, *Nano Energy*, and seven IEEE Transactions and a Guest Editor of *Wireless Communications* and *Mobile Computing*.

TIANYUAN JIA received the B.Eng. degree in telecommunications engineering from Xi'an Jiaotong–Liverpool University (XJTLU), Suzhou, China, in 2012, and the M.Sc. degree in communications and signal processing from Imperial College London, London, U.K., in 2013. He is currently pursuing the Ph.D. degree in electrical engineering and electronics with the University of Liverpool, Liverpool, U.K.

His current research interests include reverberation chamber measurement techniques, 5G over-the-air testing, propagation channel modelling and emulation, electromagnetic compatibility testing, statistical electromagnetics, and localization techniques.

XU ZHU (Senior Member, IEEE) received the B.Eng. degree (Hons.) in electronics and information engineering from the Huazhong University of Science and Technology, Wuhan, China, in 1999, and the Ph.D. degree in electrical and electronic engineering from the Hong Kong University of Science and Technology, Hong Kong, in 2003. Since 2003, she has been with the Department of Electrical Engineering and Electronics, University of Liverpool, Liverpool, U.K., where she is currently a Reader. She also has Academic Association with HIT Shenzhen, China. She has nearly 200 peer-reviewed publications. Her research interests include MIMO antennas, channel equalization, resource allocation, optimization, green communications, and so on. She has organized various international conferences as the Chair, such as the Symposium Co-Chair of the IEEE ICC 2016, ICC 2019, and Globecom 2021, the Vice-Chair of the 2006 and 2008 ICARN International Workshops, the Program Chair of the ICSAI2012, and the Publicity Chair of the IEEE IUCC-2016. She was an Editor of the IEEE Transactions on Wireless Communications, from 2012 to 2017, and a Guest Editor for a number of international journals, such as *Electronics*.